

Finite Element Model of Fatigue Fracture of Reciprocating Screw in Moulding Machine

Štěpán Major, Pavel Cyrus, and Roman Dostál

Abstract—This work is devoted to the study of fatigue degradation of some parts of moulding machine. The mechanical part of the moulding machine represents the mechanism which injects the molten plastic into the mould. The finite element analysis of fatigue damage of reciprocating screw, i.e. screw pump is discussed and compared with results obtained from fractographical analysis of damaged parts of real machine. The process of crack growth in reciprocating screw is example of fatigue of notched bar under biaxial loading. For description of biaxial loading were selected methods based on Smith–Watson–Topper and Fatemi–Socie fatigue criteria. The reciprocating screw used in this study were made from two different steels (P20+Ni and H-13 steel). The theoretical model is in a good agreement with experimental results.

Keywords—Finite element analysis, Fatigue life, moulding machine, screw pump, multiaxial criteria.

I. INTRODUCTION

MANY plastic products are manufactured using injection moulding. The injection moulding is the most commonly used manufacturing process in plastics processing. The injection moulding process requires the use of an injection machine, raw plastic material (thermoplastics are supplied typically in pelletised form), and a mould [1,2]. The injection moulding is most often used for production of thin-walled plastic parts. In many injection moulding machines are used screw-type plungers to force molten plastic into a mould cavity. This mechanism is basically an example of screw pump. This screw is placed in a heating chamber. The injection moulding machine is shown in Fig.1. The working cycle of injection machine takes typically between 2 seconds

This work was supported in research project: Specific research project SV No. 2124: “Měření únavové pevnosti kovových materiálů pod korozi”. This specific research project was sponsored by University of Hradec Králové, Faculty of Education, Department of Technical Education (Rokitanského 62, Hradec Králové 500 03, Czech Republic)

Štěpán Major is professor assistant at Department of technical education, Faculty of Education, University of Hradec Králové (Rokitanského 62, Hradec Králové 500 03, Czech Republic, s.major@seznam.cz). Štěpán Major was working as scientist at Institute of Theoretical and Applied Mechanics, Academy of Science. Štěpán Major obtained his Ph.D degree at Department of Applied Physics at University of Technology Brno.

Pavel Cyrus is ordinary professor at Department of technical education, Faculty of Education, University of Hradec Králové (Rokitanského 62, Hradec Králové 500 03, Czech Republic, pavel.cyrusl@uhk.cz).

Roman Dostál is student in master program at Department of technical education, Faculty of Education, University of Hradec Králové (Rokitanského 62, Hradec Králové 500 03, Czech Republic, roman.dostal@uhk.cz).

and 2 minutes. The working process can be divided in four stages: (1) clamping, (2) injection, (3) cooling and (4) ejection.

A. Clamping

The mould consist of two parts [2,3]. One half of mould is allowed sliding, see moveable plate in the right part of Fig.1. Prior to the injection of the material into the mould, the mould must first be securely closed by the clamping unit. The hydraulically powered clamping unit pushes the two halves of mould together and exerts sufficient force to keep the mould securely closed while the material is injected. The time required to close and clamp the mould is dependent upon the cubic capacity of mould - larger moulds will require more time and larger forces.

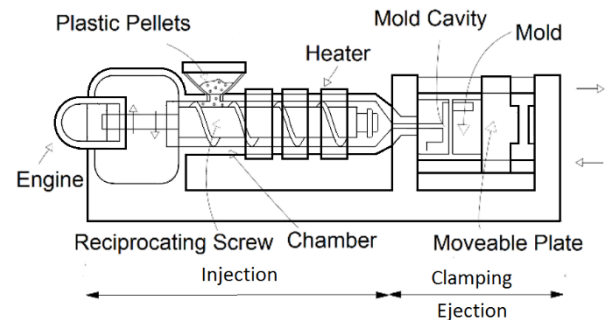


Fig. 1 Principle of the injection moulding machine with screw pump.

B. Injection

The raw plastic material is usually supplied to the manufacture in pelletised form [1,2,3]. This pellets are fed into the hopper, a large container into which the raw plastic is poured. The hopper has an open bottom, which allows the material to feed into a heated chamber with a reciprocating screw, and advanced towards the mould by the injection unit. During this process, the material is melted by heat and pressure. Process of plastic melting can be explained by the weakening of connections between polymer chains. The molten plastic is injected into the mould cavity very quickly. The amount of material that is injected is called the shot. The duration of this phase is difficult to determine accurately due to the changing flow of the molten plastic into the mould cavity. However, the injection time can be estimated by the mould volume and ratio between injection force and shot volume.

C. Cooling

The molten material that is injected in the mould cavity begins to cool as soon as it makes contact, with the interior surfaces of mould cavity. As the plastic cools, it will solidify into the desired shape. During this process, may occur uneven cooling. Uneven cooling caused shape deformation of the final product due shrinkage [1,2]. The packing of material in the injection stage allows additional material to flow into the mould and reduce the amount of visible shrinkage on the part surface. The mould cannot be opened until the required cooling time has elapsed. The cooling time can be estimated from several thermodynamic properties of the plastic. However, the most important parameter which determines cooling time is the maximum wall thickness of the product.

D. Ejection

After a certain period of cooling the plastic in the mold is stiff enough, and the plastic part can be ejected from the mould [1,2,3]. In this time, the material is so rigid, that it has not altered its shape or volume. The final product is ejected from the mould by the ejection mechanism, which is attached to the external part of the mould. When the sliding part of the mould moves forward, the mould is opened, and the ejecting mechanism is used to push the part out of the mould cavity. Force must be used to eject the part because during cooling the part adheres to the mould surface. The moulds are only seldom designed so that the product fall out of the mould only by the gravitational force. In the order to facilitate the ejection of the part, a mould release agent is often sprayed onto the surfaces of the mould cavity prior to injection of the material. Once the part is ejected, the mould can be shut by clamping and new pellets are fed in the heated chamber, whole process of melting, injecting, cooling and ejecting the final part from the mould is repeated.

In industry, the technology of injection moulding is typical for the mass production of the parts. In the case of mass production, the moulding machines are executing thousands of working- cycles per day, month or year and fatigue damage of mechanical components may occur. Fatigue fracture of reciprocating screw in melting chamber or junction of screw with motor is serious breakdown. The reliability of machine is intended by the weakest (or the most loaded) element of system. Therefore, it is necessary to study fatigue behavior of the machines. The fatigue failure of reciprocating screw is an example fracture of notched bar under torsion loading. The prediction and calculation of fatigue life of notched specimen is different from the case of smooth specimens and it requires specific approach [4,5,7,8,9,10,11].

II. FATIGUE PROCESS ANALYSIS

In the previous paragraph the principle moulding machine was described. In this paragraph fatigue damage of rotating parts of machine is analyzed. It is necessary to analyze loading and determine places of most probable fracture. The reciprocating screw and the driving shaft are loaded by torque. After large number of working cycles, some clogging of the heating chamber with remains of blowout plastic appear. This clogging

caused additional friction between the screw and internal surfaces of melting chamber. This frictional forces prevents movement of the screw and caused growth of torsional forces. These forces burden the driving shaft and the screw. The screw is loaded not only by torque, but also with axial force (tension or compression according, to the method of fixing the screw in machine). In the case of machine with two counter-rotating screws additional bending forces are present, see Fig. 2. The fracture most probably occurs at: (1) lubrication channels on the driving shaft of the reciprocating screw; (2) on the bottom of the thread of the screw pump. In the case of machine with two (or multiple) counter rotating screws and the same volume of injected plastic, the loading forces acting on individual screws are smaller, than in the case of mechanism with one reciprocating screw.

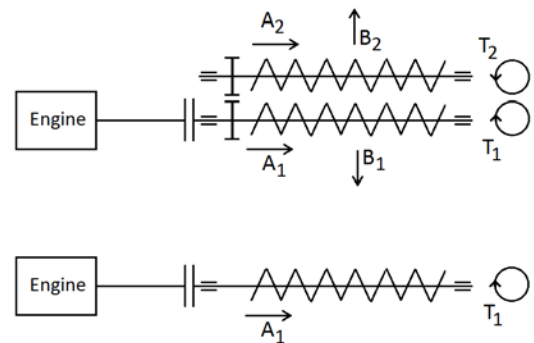


Fig. 2 Loading forces on the reciprocating screw: T_1 , T_2 torque; A_1 , A_2 axial forces and B_1 , B_2 bending forces. In the case of machine with two counter-rotating screws additional bending forces are present.

III. MATERIAL OF RECIPROCATING SCREW

The melting point of different plastics vary considerably. For example, in the case of thermoplastics such as PMMA (Poly-methyl-methacrylate) is the melting point 160 °C and, in the case Acrylic is the melting point 382°C [3]. Also, these relatively high operating temperatures can affect the fatigue resistance of the mechanical components. The creep (the creep is the tendency of a solid material to move slowly or deform permanently under the influence of mechanical stress) is generally associated with higher temperatures than the typical melting temperatures of plastics, but the temperature ranges for creep can be subdivided into three categories: (1) high temperature creep ($T > 0.6T_m$), (2) intermediate temperature creep ($0.3T_m < T < 0.6T_m$), and (3) low temperature creep ($T < 0.3T_m$). In the case of moulding machine, we can consider creep at intermediate or low temperature.

Due this reasons, some parts of the moulding machines are manufactured from heat resistant steels. For example, the high-volume moulds and tooling (such as reciprocating screws) are produced from H-13 Steel (X40CrMoV5-1) or P20+Ni Steel (40CrMnNiMo8-6-4). The typical material used for small volume moulds is for example Inconel 718 [3].

In this paper steels H-13 and P20+Ni were selected for screw manufacture. Physical properties of this materials are displayed in tables Table 1 - 4. Due to high working temperatures, the creep characteristics must be considered in analysis.

Steel	$R_{0.2\%}$ (MPa)	R_m (MPa)	$R_{C0.2\%}$ (MPa)
H-13	1280	1420	920-1000
P20+Ni	900	1020	850

Table 1. Mechanical properties for testing bar with diameter 20 mm. $R_{0.2\%}$ is Yield strength; $R_{C0.2\%}$ is compressive yield strength; R_m is tensile strength. The mechanical properties were measured at the temperature 20°C.

Steel	$R_{0.2\%}$ (MPa)	R_m (MPa)	$R_{C0.2\%}$ (MPa)
H-13	1160	1320	920-1100
P20+Ni	800	930	1000

Table 2. Mechanical properties for testing bar with diameter 20 mm. $R_{0.2\%}$ is Yield strength; $R_{C0.2\%}$ is compressive yield strength; R_m is tensile strength. The mechanical properties were measured at the temperature 200°C.

Temperature [°C]	$R_{0.2\%}$ (MPa)	E (MPa)
20	1460	210
100		205
200		198
300	1200	191
400	1100	182
500	900	173

Table 3. Parameters of H-13 steel. Relationship between the temperature and proof stress $R_{0.2\%}$, respectively elastic modulus E and temperature.

Temperature [°C]	$R_{0.2\%}$ (MPa)	E (MPa)
20	1280	208
100		204
200		197
300	1090	189
400	990	180
500	880	170

Table 4. Parameters of P20+Ni steel. Relationship between the temperature and proof stress $R_{0.2\%}$, respectively elastic modulus E and temperature.

IV. NUMERICAL MODEL OF SCREW PUMPE

One finite element model was created in ANSYS software for determination of stress-strain state in the reciprocating screw and driving shaft. Two more models are prepared for analysis of stress-strain along crack path. One of these models represents crack in the lubrication groove in the in the driving shaft (the crack initiate at the bottom U-notched bar). Other model represents cracks in the thread. The first of these cracks,

is a crack on the bottom of lubrication groove (U-notched bar). In the case of crack in the lubrication groove, the cracking plane is perpendicular to the screw axis. The second model presents a crack on the bottom of trapezoidal thread. In this case, the crack grows along the edge of the helix, with an inclination 16.5°, which corresponds to the thread pitch.

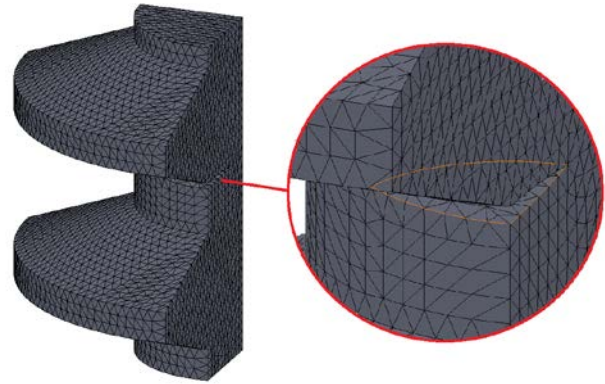


Fig. 3 Meshed finite element model of crack at the bottom of the thread. Model was simplified using symmetry.

The elliptical crack is characterized by two axes a and b . The major axis b is tangential to the thread and the secondary axis a is perpendicular to the axis of the helix, respectively to the axis of screw.

The geometry of these all models was created in the SolidWorks software. Subsequently, all these models were exported to ANSYS. Meshed models are composed from tetrahedral elements [11].

The model of crack represents the semi-elliptical crack on the bottom of the lubrication groove, respectively on the bottom of the thread of reciprocating screw, see Fig. 3. This models were simplified using symmetry. The model of crack was used for determination of stress-intensity factor along the crack-path [4,7].

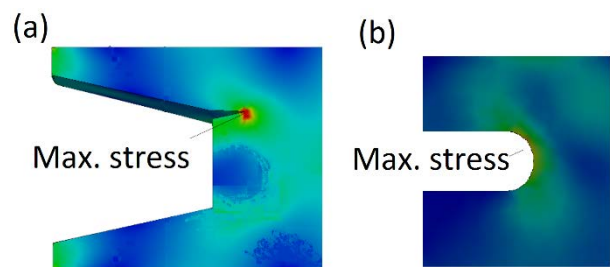


Fig. 4. Von Mises stress and its maximum: a) in crack at the bottom of the thread; b) at the bottom of lubrication groove. This two figures (a) and (b) are not in the same scale.

The finite element model allows to determine the distribution of the von Mises stress at the bottom of the thread at the point maximal loading was calculated. The distribution of Von Mises stress at the bottom of the thread is shown at the Fig. 4.

V. FATIGUE LIFE CALCULATION

The growth of crack in the bar under external load can be simulated by mathematical model based on approach proposed by Navarro et al. [12,13,14,15]. In general, the process of fatigue damage can be divided in two stages: Initiation phase and Propagation phase [4]. In the newer literature, we can find partition of process in four stages: Crack nucleation; Stage I growth; Stage II growth, Ultimate ductile failure [4]. In mathematical description is Initiation phase equal to Stage I growth and Propagation phase is equal to Stage II growth. This stages differ in mechanism of crack growth. Stage I crack growth is strongly affected by slip characteristics, microstructure dimensions, stress level, extent of near tip plasticity. In this case the crack growth along the surface of the metallic grain. Stage II growth is characterised by growth through metallic grains. The Stage I goes in Stage II when the crack reaches a certain crack length a_m (subscription m means microstructural). Most models of fatigue fracture need predefined threshold length of crack, that distinguishes between Stage I and Stage II.

Mathematical model based on Navarro approach is exceptional, because this model does not need predefined threshold length of crack. For modeling of fatigue process, it is necessary to determine σ - N curve or a - N [12,14,15]. The reciprocating screw is under multiaxial loading, see Fig. 2. The uniaxial loading can be assessed as multiaxial loading with some components equal to zero (loads B_1 and B_2 in Fig.2). In this case the curve σ - $N_{i,FR}$ is expressed by parameters obtained from any multiaxial fatigue criteria. Total number of cycles to the final failure can be expressed [12,14,15]:

$$N_f(D_{Multia}) = N_i(D_{Multia}, a) + \int_a^{a_{FR}} \frac{da}{f(a)} \quad (1)$$

The length a_{FR} is the crack length at the time of final failure. The D_{Multia} is damage parameter obtained from some multiaxial criteria [4,5,6,7,8,9,14,16]. Mathematical model used Paris-Erdogan law for description crack growth. The Paris-Erdogan equation describes the relationship between the stress intensity factor SIF and increment of the crack length Δa . The stress intensity factor SIF at the forehead of crack is depending on the distance from the surface (in our case bottom of the thread or bottom of lubrication groove).

The determination of SIF at the front of the crack is based on J -integral method [4,7,8]. The SIF is a function of the increment crack length Δa . This relation between SIF and length of increment crack Δa can be determined by repeated simulations. The length of the crack at the beginning of simulation was set to 5 μm . This length is apparently much smaller than the threshold length of crack for the propagation phase.

The basic form of Paris law is very simple, but it has some disadvantages. Especially, this law does not take the crack growth threshold into account. Therefore, more complicated relationship was used

$$\frac{da}{dN} = C \left(\Delta K^m - (\Delta K_{th,Long} f_{micro}(a, P_{KT}))^m \right), \quad (2)$$

This relationships is introducing a threshold for long cracks, $\Delta K_{th,Long}$. The function $f_{micro}(a, P_{KT})$ describes the influence microstructural parameters on crack growth speed at the Stage I of fatigue process.

$$f_{micro}(a, P_{KT}) = \left(\frac{a^{P_{KT}}}{a^{P_{KT}} + d_0^{P_{KT}} - l_0^{P_{KT}}} \right)^{\frac{P_{KT}}{2}}. \quad (3)$$

The power parameter P_{KT} is obtained from Kitagawa–Takahashi diagram [17]. The parameter a_0 is the El Haddad parameter [18] and l_0 is the average distance to the first microstructural barrier. The curve σ - $N_{i,FR}$ was obtained from Eq. 2.

Another phase of the fatigue process is described by the curve a - N_i . In the Eq. 1, damage parameter D_{Multia} is used. This parameter can be obtained from different types of multiaxial fatigue criteria. The Fatemi-Socie and Smith–Watson–Topper criteria was chosen in our work. In the case of Fatemi-Socie criteria, the damage parameter is written as [4,7,8]:

$$FS = \frac{\Delta \gamma_{max}}{2} \left(1 + k \frac{\sigma_{max}}{R_m} \right). \quad (5)$$

Variables used in this relationship: $\Delta \gamma_{max}$ is the shear strain increment in the plane where it has maximum value, k is a constant (it is obtained from the fatigue tests), σ_{max} is the normal stress perpendicular to the plane where is the maximum shear strain, and R_m is the yield strength.

The Smith–Watson–Topper criteria [16] has an important advantage. It was successfully used for description the fatigue behavior of processed metals at high working temperatures (however, under temperature typical for creep). This criterion defined by Smith et al. [16] is defined as the maximum, among all possible directions, of the strain amplitude multiplied by the normal maximum stress [14,16]:

$$SWT = \left(\frac{\sigma_{max} \Delta \varepsilon}{2} \right)_{max}. \quad (6)$$

The complete fatigue life can be obtained by merging of a - N_i curve and a - N_{FR} curve. The complete fatigue life can be obtained by merging of a - N_i curve (number of cycles to length) and a - N_p curve (number of cycles to rupture), if both curves are known, they can be merged [12,13,14]. Merged curves can be used for description of the entire fatigue life of specimen. This curve for total life of screw is shown in Fig. 5. Red colour: screw is manufactured from P20+Ni steel, crack initiated in lubrication groove. Green colour: steel P20+Ni, crack initiated at the bottom of thread. Blue colour: Screw was manufactured from H-13 steel, crack initiated in lubrication

groove. Yellow colour: crack initiated at the bottom of thread. The thin curves are the partial curves $a-N_i$ and $a-N_{FR}$. These curves are shown only in one case for clarity. These curves were obtained using SWT criteria. Brown and purple curves were obtained by FS criteria. Brown colour indicates initiation of crack in the lubrication groove, and the purple colour represents the crack at the bottom of the thread. This curve was used for comparison these two methods. In the figure are black curves, this curves were obtained by experiments. This black curves are prepared according fractographical analysis. These allows distinguish between propagation and initiation phase. From this picture is clearly visible, that the initiation life is smaller than propagation life. The curve obtained by FS criteria gives inferior results to the SWT criteria. This means that SWT criteria is better describing metals response on loading by higher temperatures.

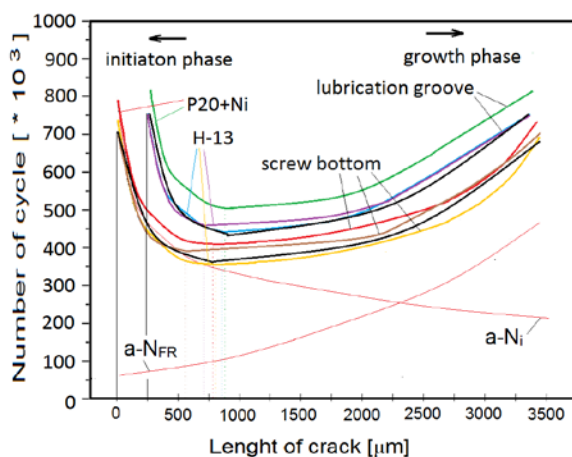


Fig. 5. Theoretical fatigue curves for reciprocating screw. Full description of graph is in the text.

VI. RESULTS AND DISCUSSION

Theoretical fatigue curves for temperature 300°C are shown in Fig. 5. Also, the fatigue experiments for trapezoidal and U-notched bars are shown in this figure. Bars with U notch have same behaviour as lubrication groove and bars with trapezoidal notch (angle 30°) corresponds to the bottom of thread. Because lubrication groove is in region with lower working temperatures, the results for the U-notched specimens are very closed to the model. Curves obtained for material H-13. The model of fatigue damage of screws pump is described in this paper. Comparison of experimental and theoretical model shows considerable agreement with reality. The lowest point of fatigue life curve is point where “initiation” curve and “propagation” curve were merged together. This point divided fatigue process on initiation and propagation stage. The initiation stage is shorter than the propagation phase, see. Fig.5. The initiation phase represents about 20% of whole fatigue life. If the prediction obtained using Fatemi-Socie criteria (damage parameter FS obtained from Fatemi-Socie criteria) is compared with prediction in which SWT damage parameter (damage parameter obtained from Smith–Watson–Topper multiaxial criteria) was used, the experimental results are more distant from theory in case of FS damage parameter. The Smith-Watson-Tooper criteria more suitable for description of fatigue process at high temperatures, such as temperatures in working chamber of moulding machine.

ACKNOWLEDGMENT

This research has been supported by: Specific research project No. 2124 „Měření únavové pevnosti kovových materiálů pod korozi“ University of Hradec Králové, Faculty of Education.

REFERENCES

- [1] D. M. Bryce, *Plastic Injection Moulding: Manufacturing Process Fundamentals*, SME, 1996.
- [2] R. H. Todd, H. Robert, D.K Allen, L. Alting, *Manufacturing Processes Reference Guide*. Industrial Press, Inc. 1994.
- [3] R. A. Malloy, *Plastic Part Design for Injection Moulding*. Munich Vienna New York: Hanser, 1994.
- [4] D. F. Socie, G. B. Marquis, *Multiaxial fatigue*. SAE Int., Warrendale, 2000.
- [5] J. Schijve, *International Journal of Fatigue*, 25 (8), 2003, pp. 679-702.
- [6] Š. Major, J. Papuga, J. Horníková, J. Pokluda, *Strength of Materials*, Vol.1, January 2008, pp.64-66.
- [7] A. Fatemi, P. Kurath, *Journal of Engineering Materials and Technology, Transactions of the ASME*, 110 (4), pp. 380388.
- [8] D. F. Socie, J. Morrow, W.-C. Chen, *Engineering Fracture Mechanics*, 11 (4), pp. 851-859.
- [9] Š. Major, J. Valach, Analysis of the effectiveness of fatigue criteria for biaxial loading of notched specimens, *EAN 2014 - 52nd International Conference on Experimental Stress Analysis*, 2014.
- [10] Š. Major, S. Hubálovský, V. Kocour, J. Valach, *Applied Mechanics and Materials*, No. 732, 2015, pp. 63-70.
- [11] J.N. Reddy, *An Introduction to the Finite Element Method (Third ed.)*. McGraw-Hill, 2006
- [12] J.M. Ayllón, C. Navarro, C., Vázquez, J., Domínguez, *Engineering Fracture Mechanics*, No.123 2014, pp. 34-43.
- [13] C. Navarro, J. Vázquez, J. Domínguez, *Engineering Fracture Mechanics*, 2011, pp. 1590-1601.
- [14] C. Navarro, S. Muñoz, J. Domínguez, *Tribology International*, 39 (10), 2006, pp. 1149-1157.
- [15] Š. Major, V. Kocour, P. Cyrus, *Frattura ed Integrità Strutturale*, Vol. 10, Issue 35, 2016, pp. 379-388.
- [16] K. N. Smith, P. Watson, T. H. Topper, *Journal of Materials*, ASTM, Vol. 5, No. 4, Dec. 1970, pp. 767-778.
- [17] H. Kitagawa, S. Takahashi, S., In: *Proceedings of the Second International Conference on Mechanical Behavior of Materials*, Metals Park, OH: ASM; 1976, pp. 627-31
- [18] M.H. El Haddad, T.H. Topper, K.N. Smith, *Engineering Fracture Mechanics*, Vol.11 1979, pp. 573-584.